

# The Effect of Quadrature Modulator and Demodulator Errors on Adaptive Digital Predistorters for Amplifier Linearization

James K. Cavers, *Member, IEEE*

**Abstract**—Imperfections in quadrature modulators and demodulators—gain and phase imbalance and dc offset—have a crippling effect on amplifier linearization circuits, a fact that has previously been noted experimentally. This paper is the first analysis of these effects on an adaptive predistorter. The primary result is an expression that provides an explicit tradeoff among intermodulation power, accuracy of the quadrature modulator and demodulator, and speed of adaptation. Another useful result is a simple and easily measured error figure for quadrature modulators and demodulators.

**Index Terms**—Amplifiers, linearization, transceivers.

## I. INTRODUCTION

WITH THE increasing importance of spectral efficiency in mobile communications, linearity of the power amplifier has become a critical design issue for nonconstant envelope modulations. Several methods for linearization have been investigated in recent years, but, except for a very few studies [1]–[3], the effect on linearization circuits of errors in the quadrature modulator and demodulator has all but been ignored. This is a considerable oversight, because even the small errors encountered in good commercially available devices can produce a large intermodulation (IM) error at the amplifier output, to the point that the expense and design effort of linearization is essentially wasted.

To date, the only substantial analysis [1] dealt with the effect of quadrature modulator errors (gain imbalance, phase imbalance, and dc offset) on a static, previously optimized predistorter, and with polynomial characteristics for both the amplifier and predistorter. It demonstrated substantial regrowth of the IM skirts even for small errors.

The present paper is a full analysis of the problem: it includes the effect of adaptation in the predistorter; it does not constrain the amplifier to have polynomial characteristics; and it quantifies the effect of errors in both the quadrature modulator used in the forward path and the quadrature demodulator used in the feedback path. The principal result is an expression that gives the IM power at the amplifier output as a function of the quadrature modulator and demodulator errors and the speed of adaptation (and, of course, the amplifier characteristic). This

Manuscript received September 26, 1995; revised May 17, 1996 and June 24, 1996. This work was supported in part by a grant from Tait Electronics Ltd., Christchurch, New Zealand.

The author is with the School of Engineering Science, Simon Fraser University, Burnaby, B.C., V5A 1S6 Canada (e-mail: cavers@sfu.ca).

Publisher Item Identifier S 0018-9545(97)03127-7.

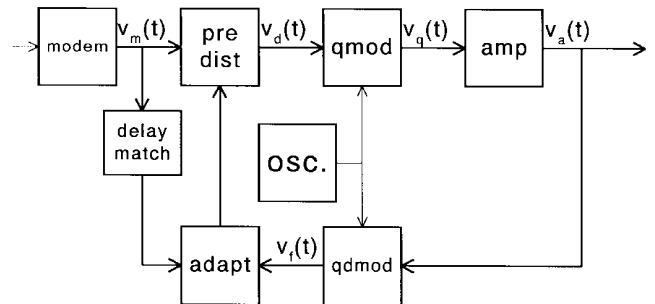


Fig. 1. Organization of an adaptive digital predistorter.

allows the designer to estimate the required level of correction of these errors according to the system specifications. Since the expression is relatively complex, an approximation that can be evaluated on a hand calculator and is accurate to about 1.5 dB (close enough for most calculations of IM power) is also provided. A second significant result of the analysis is a simple and easily measured error figure of a quadrature modulator or demodulator.

Because of the complexity of the problem—nonlinearities interacting with memory—most of the results provide only IM power, not spectrum. However, we show that the IM power due to predistorter adaptation jitter is white. Further, for the special case of a static previously optimized predistorter and a general amplifier nonlinearity, the analysis demonstrates how the quad mod errors affect the regrowth of the IM spectrum.

## II. BASIC MODELS

### A. Overall Structure

Fig. 1 shows the organization of an adaptive predistortion circuit. All signals are treated as complex baseband, and denoted by  $v(t)$ , with a subscript to identify the precise signal or location in the circuit. The instantaneous power, or squared magnitude, is indicated by  $x(t)$ , and its average over the modulation ensemble is denoted by  $P$ , both with subscripts. For example,  $v_a(t)$  is the complex envelope of the amplifier output,  $x_a(t) = |v_a(t)|^2$ , and  $P_a = E[x_a(t)]$ .

The forward branch consists of a complex baseband predistorter, a quadrature modulator to convert its output to RF and the power amplifier, modeled as a memoryless nonlinearity. Ideally, the quadrature modulator (quad mod) is a unity gain

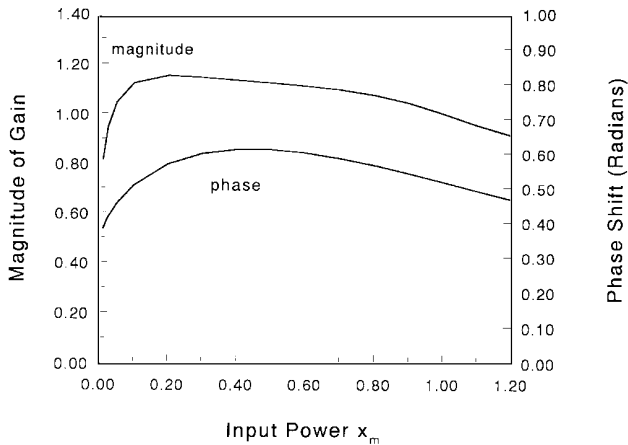


Fig. 2. Typical class AB amplifier characteristics.

block and the predistorter is the precise inverse of the power amplifier nonlinearity, so that the combination of the three is a simple linear gain  $K$ . In reality, the predistorter and quad mod have small errors, so that the amplifier output  $v_a(t)$  contains IM and other errors, given by

$$v_{ae}(t) = v_a(t) - Kv_m(t) \quad (1)$$

where  $v_m(t)$  is the modulation input. The primary results of this paper are expressions for  $x_{ae}(t)$  and  $P_{ae}$  for an adaptive predistorter.

Adaptation of the predistorter is achieved by comparing the fed back amplifier output  $v_f(t)$  with the desired amplifier output  $Kv_m(t)$  and adjusting the predistorter parameters to minimize some measure of the difference

$$v_{fe}(t) = v_f(t) - Kv_m(t). \quad (2)$$

The delay element matches delays around the loop containing the amplifier. We assume it to be perfectly adjusted, so that loop delay has no effect on linearization accuracy. The adaptation itself can be a relatively slow background process.

### B. Power Amplifier

The power amplifier is characterized by a level-dependent complex gain  $G(x)$ , so that its output is given by

$$v_a(t) = v_q(t)G[x_q(t)] \quad (3)$$

where  $v_q(t)$  is the output of the quadrature modulator. The complex gain of a typical Class AB amplifier is shown in Fig. 2 as magnitude (AM/AM) and phase (AM/PM), where input and output power have both been normalized to unity at saturation. The reduced gain at saturation and cutoff are clearly evident, as are the phase shifts in these regions. We will also use the derivative of the complex gain, denoted by

$$G'(x) = \frac{dG(x)}{dx}. \quad (4)$$

In general, power amplifiers also exhibit dynamic (i.e., memory) effects, particularly in regions of rapid gain change like saturation and cutoff. These effects are not represented by the complex gain model, and therefore cannot be corrected

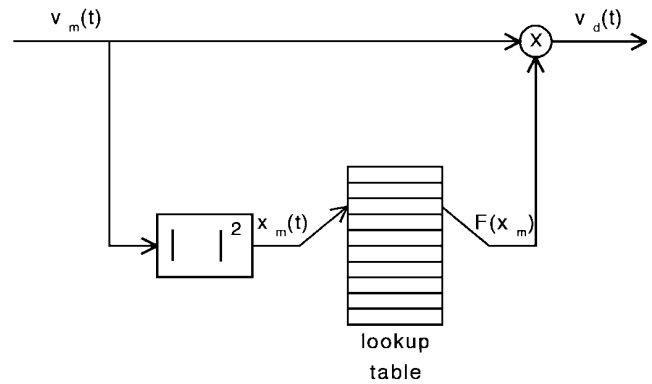


Fig. 3. Complex gain predistorter with LUT.

by the complex gain predistorter. However, for bandwidths of the size accessible to digital predistortion, memory effects are considerably smaller than the basic memoryless distortion produced by level-dependent complex gain, as shown by successful implementations [7], [8]. Moreover, we show below that uncorrected quadrature modulator and demodulator errors further raise IM floors. For these reasons, amplifier memory has been ignored.

### C. Predistorter

The predistorter is another level-dependent complex gain  $F(x)$ , with output given by

$$v_d(t) = v_m(t)F[x_m(t)]. \quad (5)$$

If the quadrature modulator was a perfect unity gain device, we could identify  $v_q(t)$  with  $v_d(t)$ , and the optimum predistorter characteristic, denoted by  $F_o(x)$ , would satisfy

$$F_o(x_m)G[x_m|F_o(x_m)]^2 = K \quad (6)$$

which follows from (3) and (5). We will show later that  $F_o(x)$  is the mean value of the adaptation, even in the presence of quad mod and quad demod errors.

Note that the amplifier output power cannot exceed its saturation value. The best possible characteristic of the combined predistorter and amplifier is therefore that of a limiter having an output signal proportional to the input signal with slope  $K$ , up to a limiting value, after which the predistorter supplies AM/PM correction only. The effect of the gain  $K$  is simply to change the range of the input, that is, the input power  $x_m$  at which the amplifier saturates.

The predistorter is assumed to be implemented as a lookup table (LUT) of complex gain values [4], indexed by the squared magnitude  $x_m$ , as shown in Fig. 3. It is also possible to index by magnitude, or any other monotonic function of magnitude, depending on the regions of amplifier characteristic that need the greatest accuracy of representation. However, these considerations do not enter the analysis of the present paper.

### D. Quadrature Modulator

Fig. 4 gives an expanded view of the physical quadrature modulator, and Fig. 5 illustrates the model used in this paper.

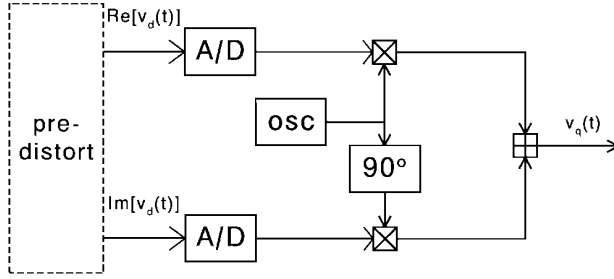


Fig. 4. Physical structure of the quadrature modulator.

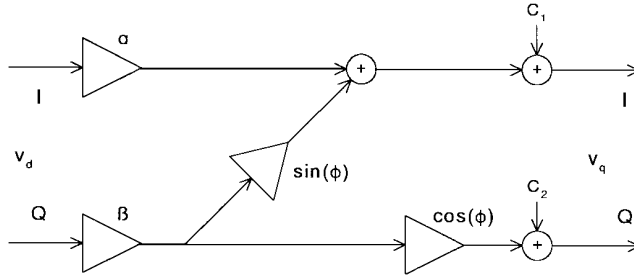


Fig. 5. Analytical model of the quadrature modulator.

We are concerned with three primary departures from ideality. Phase imbalance  $\phi_m$  is the amount by which the sine carrier departs from its ideal  $\pi/2$  phase behind the cosine carrier. Gain imbalance  $\varepsilon_m$  depends on the ratio of amplitude gains  $\alpha$  in the cosine branch and  $\beta$  in the sine branch and is given by

$$\varepsilon_m = \frac{\alpha}{\beta} - 1. \quad (7)$$

Ideally,  $\alpha = \beta$ , so that  $\varepsilon_m = 0$ . In order not to confuse gain imbalance with an overall change in power [2], we will constrain the branch amplitude gains to be

$$\alpha = (1 + \varepsilon_m) \sqrt{\frac{2}{2 + 2\varepsilon_m + \varepsilon_m^2}}$$

$$\beta = \sqrt{\frac{2}{2 + 2\varepsilon_m + \varepsilon_m^2}}. \quad (8)$$

The third nonideality is dc offset, produced by the true dc offset in D/A converters and active reconstruction filters and by carrier feedthrough to the quad mod output.

Previous analyses have used matrix [2] or conjugate vector [1] representations of the quad mod. The latter is generally more convenient for analysis. We therefore write the complex envelope of the quad mod output as

$$v_q(t) = Av_m(t) + Bv_m^*(t) + C \quad (9)$$

where

$$A = \frac{1 + \cos(\phi_m) + \varepsilon_m - j \sin(\phi_m)}{\sqrt{4 + 4\varepsilon_m + 2\varepsilon_m^2}} \quad (10)$$

and

$$B = \frac{\varepsilon_m \cos(\phi_m) + j \sin(\phi_m)}{\sqrt{4 + 4\varepsilon_m + 2\varepsilon_m^2}} \quad (11)$$

and  $C$  is the complex dc offset.

With good analog design, the gain and phase imbalance errors  $\varepsilon_m$  and  $\phi_m$  are relatively small, typically about 3% and  $3^\circ$  or less, respectively. With such small values, we can adopt the first order approximations

$$A \approx 1$$

$$B \approx \frac{\varepsilon_m + j\phi_m}{2} \quad (12)$$

so that

$$v_q(t) \approx v_d(t) + Bv_d^*(t) + C. \quad (13)$$

From (13), it is clear that  $|B|^2$  has a simple interpretation as the power ratio of undesired to desired images when the input to the quad mod is the offset tone  $\exp(j2\pi f_o t)$ . Further,  $|C|^2$  is the power in a tone at dc (i.e., center channel). Because they play a significant role in our analysis, we define the image suppression ratio (ISR) and the dc suppression ratio (DSR) of the quadrature modulator as

$$\text{ISR}_m = |B|^2$$

$$= \frac{\varepsilon_m^2 + \phi_m^2}{4}$$

$$\text{DSR}_m = \frac{|C|^2}{x_m}. \quad (14)$$

Note that these quantities are easily measured with a spectrum analyzer when the quad mod input is a single offset tone: DSR is the residual carrier level, and ISR is the level of the image on the opposite side of the carrier, both of them relative to the level of the tone.

### E. Quadrature Demodulator

The quadrature demodulator is constructed much like a quadrature modulator in reverse, recovering the complex envelope of its bandpass input. It, too, has gain and phase imbalances  $\varepsilon_d$  and  $\phi_d$ . The complex dc offset  $c$  in its output is due to mixing of the local oscillator (LO) signal with itself,  $1/f$  noise in the mixers, and true dc offsets in active antialiasing filters and A/D converters. Because it parallels the model of the quad mod so closely, we simply summarize its behavior by

$$v_f(t) = av_a(t) + bv_a^*(t) + c$$

$$\approx v_a(t) + bv_a^*(t) + c \quad (15)$$

where

$$b \approx \frac{\varepsilon_d + j\phi_d}{2}. \quad (16)$$

Its image suppression ratio  $\text{ISR}_d$  and dc suppression ratio  $\text{DSR}_d$  are defined like the analogous quantities (14) in the modulator.

### F. Adaptation Algorithm

Adaptation of the predistorter is based on comparison of paired samples of desired and fed back amplifier outputs. Because the predistorter is constructed as an LUT, only the table entry associated with the magnitude  $x_m$  of the modulation sample is adjusted in response to a given sample

pair. Conversely, a table entry is adjusted only when the signal trajectory passes through the corresponding amplitude level.

For any signal power  $x_m$ , we find the root  $F_o$  of (6) by the method of successive substitutions [5], for which an iteration is

$$F(x_m, i+1) = \frac{K}{G[x_m|F(x_m, i)|^2]} \quad (17)$$

where  $i$  is the iteration index and  $F$  has been given a second argument. The Appendix shows that convergence to  $F_o$  is guaranteed in the neighborhood of the root if

$$2Kx_m \frac{|G'_o| |F_o|}{|G_o|^2} < 1 \quad (18)$$

where  $G_o$  and  $G'_o$  denote amplifier characteristics corresponding to the optimum value  $F_o$ , and are given by

$$\begin{aligned} G_o &= G[x_m|F_o(x_m)|^2] \\ G'_o &= G'[x_m|F_o(x_m)|^2]. \end{aligned} \quad (19)$$

Thus we can be more confident of convergence in regions where the complex gain varies slowly or the signal level is small, and divergence, if it occurs, is most likely to be near saturation. If we ignore temporarily the errors in the quad mod and demod, treating them as unity gains, we can identify  $v_q$  with  $v_d$  and  $v_f$  with  $v_a$ . Substitution of (3) and (5) into (17) then yields

$$\begin{aligned} F(x_m, i+1) &= F(x_m, i) \frac{Kv_m(i)}{v_a(i)} \\ &= F(x_m, i) \left[ 1 - \frac{v_{ae}(i)}{v_a(i)} \right] \end{aligned} \quad (20)$$

where the second equality comes from (1). This iteration was also used in [3]. As we shall see, however, errors in the quad mod and demod necessitate averaging of (20) over many iterations. Accordingly, we use the update

$$F(x_m, i+1) = F(x_m, i) \left[ 1 - s \frac{v_{ae}(i)}{v_a(i)} \right] \quad (21)$$

where  $s \ll 1$  is a small positive step size parameter. The Appendix demonstrates that, though  $s$  may affect the speed of convergence, it does not change the convergence condition (18). Finally, recalling that we have available  $v_f$  instead of  $v_a$ , we rewrite (21) to obtain the iteration update used in the remainder of the analysis

$$F(x_m, i+1) = F(x_m, i) \left[ 1 - s \frac{v_{fe}(i)}{v_f(i)} \right] \quad (22)$$

where  $v_{fe}$  is defined in (2).

The iteration (22) is reasonably representative. For example, we could equally well have used geometric averaging of (20), by

$$\begin{aligned} F(x_m, i+1) &= F(x_m, i) \left[ \frac{Kv_m(i)}{v_a(i)} \right]^s \\ &= F(x_m, i) \left[ 1 - \frac{v_{ae}(i)}{v_a(i)} \right]^s. \end{aligned} \quad (23)$$

For small  $|v_{ae}|/|v_a|$ , (23) reduces to our intended iteration (21). Moreover, (23) is closely related to another published iteration [6]–[8], given by

$$\begin{aligned} &\arg[F(x_m, i+1)] \\ &= \arg[F(x_m, i)] + s\{\arg[v_m(i)] - \arg[v_a(i)]\} \\ &|F(x_m, i+1)| \\ &= |F(x_m, i)| + s[K|v_m(i)| - |v_a(i)|]. \end{aligned} \quad (24)$$

This phase iteration is identical to (23). Some manipulation also shows that magnitude increment in this iteration is approximately  $|v_m G_o|$  times that in (23); that is, predistorter table entries associated with larger amplitudes near saturation receive large updates, while entries associated with small amplitudes near cutoff receive very small updates. In any case, the links among the update methods suggest that (22) is representative, as well as tractable.

### III. STATIC ERROR IN AMPLIFIER OUTPUT

In this section, we obtain the error in the amplifier output as a function of the quad mod errors and any misadjustment error in a static (i.e., nonadaptive) predistorter.

#### A. Linearized Model of Amplifier Error

We will suppose the predistorter characteristic to have a perturbation  $\delta F$  that is small compared with  $F_o$ , so that

$$F = F_o + \delta F \quad (25)$$

where the explicit dependence on  $x_m$  has been suppressed to simplify notation. Combining (5) and (13), we have the quad mod output, to first order in the small errors  $\delta F$  and  $B$ , as

$$v_q \approx v_m F_o + v_m \delta F + B v_m^* F_o^* + C. \quad (26)$$

Considering that the dc offset is small compared with the modulation,  $|C| \ll |v_m|$ , we have the first-order approximation of the squared magnitude of  $v_q$

$$x_q \approx x_m |F_o|^2 + 2x_m \operatorname{Re}[F_o^* \delta F] + 2\operatorname{Re}[B^* F_o^2 v_m^2 + C^* F_o v_m], \quad (27)$$

The quality of approximation is excellent in (26), and in (27) it is very good for signal amplitudes greater than about ten times the dc offset. In both equations, the leading term is the ideal value, and the remaining terms are perturbations caused by predistorter and quad mod errors.

To calculate the amplifier output, we note that the perturbation in  $x_q$  causes a perturbation  $\delta G$  in the amplifier complex gain away from  $G_o$  of (19). Using (27) and a first-order Taylor expansion of  $G(x)$ , we have

$$\delta G \approx \{2x_m \operatorname{Re}[F_o^* \delta F] + 2\operatorname{Re}[B^* F_o^2 v_m^2 + C^* F_o v_m]\} G'_o \quad (28)$$

where  $G'_o$  is defined in (19). From (3), then, we obtain the first-order approximation to the amplifier output as

$$\begin{aligned} v_a &= (v_m F_o + \delta v_q)(G_o + \delta G) \\ &\approx v_m F_o G_o + \delta v_q G_o + v_m F_o \delta G. \end{aligned} \quad (29)$$

Since  $F_o G_o = K$ , we have the amplifier output error  $v_{ae}$  as the last two terms of (29). Substituting (26) and (28), we have

$$v_{ae} \approx v_{aeF} + v_{aeq} \quad (30)$$

where

$$v_{aeF} = v_m \{ G_o \delta F + 2x_m F_o G_o' \operatorname{Re} [F_o^* \delta F] \} \quad (31)$$

is the component of the error due to misadjustment of the predistorter when the quad mod is perfect, and

$$v_{aeq} = (Bv_m^* F_o^* + C)G_o + 2v_m F_o G_o' \cdot \operatorname{Re} [B^* F_o^2 v_m^2 + C^* F_o v_m] \quad (32)$$

is the component due to quad mod errors when the predistorter is perfect. In the remainder of the analysis, we will deal with the two terms separately.

The approximation (30) is very good. For combinations of imbalance errors of 3% and 0.03 radians and dc offsets of 3% of saturating signal amplitude (which we will term the 3/3/3 level of error), the error in (30) is typically less than about 3% of the true value, even for very low signal amplitudes.

### B. Quad Mod Error and Spectral Regrowth

The component  $v_{aeq}$  of amplifier output error due to quad mod error can be taken a little further. We can rewrite (32) as

$$v_{aeq} = Bv_d^* G(x_d) + 2v_d G'(x_d) \operatorname{Re} [B^* v_d^2] + CG(x_d) + 2v_d G'(x_d) \operatorname{Re} [C^* v_d] \quad (33)$$

which can be seen as a regrowth of IM spectra. If  $v_d$  is zero mean and circularly complex (i.e.,  $E[v_d^m (v_d^*)^n] = 0$  for  $m \neq n$ ), as usual, it is straightforward to show that the first two terms are uncorrelated with the second two. Consequently, the power spectrum of  $v_{aeq}$  is the sum of one spectrum weighted by  $|B|^2$  and another weighted by  $|C|^2$ . That is, the two components of spectral regrowth are proportional to the image suppression ratio  $ISR_m$  and the dc suppression ratio  $DSR_m$  (14).

Further insight can be gained by considering both the amplifier and predistorter characteristics as a dominant linear component (constant gain), plus a smaller nonlinear component with level-dependent gain (typically 25 dB or more below the linear component), an approach developed successfully in [9]. Thus the predistorter output can be written as

$$v_d = K_F v_m + v_{IMd} \quad (34)$$

where  $K_F$  is the linear component of predistorter gain and  $v_{IMd}$  is the nonlinear distortion at the predistorter output. Also the amplifier complex gain can be written

$$G(x_d) = K_G + G_{IM}(x_d) \quad (35)$$

where  $K_G$  is the linear component of the gain and  $G_{IM}$  is the level-dependent component that gives rise to distortion. The linear gains can be determined by correlation of inputs and

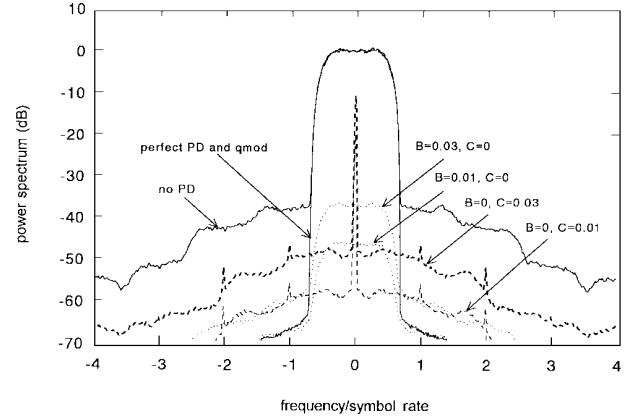


Fig. 6. Spectral regrowth due to quadrature modulator errors with static predistorter.

outputs, as in [10]. Selectively substituting (34) and (35) into (33) gives

$$v_{aeq} = BK_G K_F^* v_m^* + BK_G v_{IMd}^* + BG_{IM}(x_d) v_d^* + 2v_d G'(x_d) \operatorname{Re} [B^* v_d^2] + CK_G + CG_{IM}(x_d) + 2v_d G'(x_d) \operatorname{Re} [C^* v_d]. \quad (36)$$

In (36), the first  $B$  term (a spectrally reflected replica of  $v_m$ ) and the first  $C$  term (a tone at the center of the channel) dominate the remainder of their respective terms. However, they both fall in the signal band and do not contribute to adjacent channel interference. The remaining components have bandwidth wider than the original modulation. Here we can identify a difference in the IM spectra resulting from noise-like input signals and data signals. With the former, all spectral components of (36) are continuous in frequency. In contrast, data signals are cyclostationary, so that  $x_m$  and its powers typically contain discrete tones at multiples of the symbol rate; in fact, the tones in  $x_m$  are frequently used for timing recovery. Thus  $G_{IM}(x_d)$  in the second  $C$  term of (36) contributes such tones, and their power is proportional to  $|C|^2$ . All other terms have continuous spectra. We also note from (36) that the continuous spectra decrease at various rates with decreasing  $v_m$ , but that the discrete components are largely unaffected by decreasing signal power, and therefore become increasingly prominent. Beyond these observations, it is difficult to obtain general results about spectral regrowth without resorting to computation. On the other hand, analytical results for the regrowth of IM spectrum resulting from quad mod error are available [1] for the particular case of polynomial models for the amplifier and the predistorter, and they too show that the total output spectrum is a linear combination of elementary spectra.

Fig. 6 presents the amplifier output spectra for  $\pi/4$  DQPSK with 35% rolloff under several conditions. The desired linear gain was set to  $K = 1$ , so that saturation was reached at  $x_m = 1$ . The average modulation power was backed off to 3.1 dB less than saturating power to ensure that overload of the limiter characteristic of the linearized amplifier produced no appreciable IMD (note that input and output

backoffs are equal with linearization). For reference, one curve shows the output with no predistortion; that is, when the amplifier input is  $K_F v_m$ . Other curves illustrate the output error spectrum for perfect predistortion followed by various levels of quad mod error. Because of the normalization,  $C$  values can also be interpreted as dc offset amplitudes relative to the saturating amplitude. The output error spectra demonstrate proportionality to  $|B|^2$  and  $|C|^2$ , as predicted, and the dominance of the inband components  $BK_G v_m^*$  and  $CK_F$ , as well as the fact that offset generally has a more severe effect than imbalances. They also illustrate tones at multiples of the symbol rate due to cyclostationarity of the signal. It is clear that even relatively small amounts of quad mod error compromise the improvement gained through predistortion.

#### IV. JITTER-INDUCED ERROR IN AMPLIFIER OUTPUT

In this section, we turn to the component  $v_{aeF}$  of amplifier output error (30) due to misadjustment of the predistorter. In the adaptive configuration at hand, misadjustment is in the form of jitter caused by quad mod and demod errors. We derive the error power and show that this component of the error has a flat spectrum.

The strategy is to condition the analysis on the input level, and obtain a linear stochastic difference equation as an approximation of the iteration in the neighborhood of the optimum value  $F_o$ . Since such equations are well understood, we can obtain the jitter variance and the dynamics of convergence as explicit functions of input level. Subsequent averaging with respect to input signal level completes the calculation.

##### A. Linearized Model of Feedback Error

The error in the feedback signal  $v_f$  can be obtained to first order by combining (1), (15), (30), and (31) to give

$$v_f \approx K v_m + v_m \{G_o \delta F + 2x_m F_o G'_o \operatorname{Re} [F_o^* \delta F]\} + u \quad (37)$$

where

$$u = (B v_m^* F_o^* + C) G_o + 2v_m F_o G'_o \cdot \operatorname{Re} [B^* F_o^2 v_m^2 + C^* F_o v_m] + b K v_m^* + c \quad (38)$$

acts as a noise term produced by the quad mod and quad demod errors. From (2), the error  $v_{fe}$  equals the last two terms in (37). As in (30), the approximation of the error  $v_{fe}$  is very good.

##### B. Linearized Model of Adaptation

The predistorter adaptation dynamics are seen more clearly in terms of the misadjustment  $\delta F$ . Substituting (25) into (22) gives, to first order

$$\delta F(x_m, i+1) \approx \delta F(x_m, i) - s F_o \frac{v_{fe}(i)}{v_f(i)} \quad (39)$$

for an iteration of the entry in the LUT corresponding to signal magnitude  $x_m$ . Further substitution of (2) and series expansion

of the denominator gives

$$\delta F(x_m, i+1) = \delta F(x_m, i) - s F_o \frac{v_{fe}(i)}{K v_m} \cdot \left\{ 1 + \frac{v_{fe}(i)}{K v_m} - \left[ \frac{v_{fe}(i)}{K v_m} \right]^2 + \dots \right\}. \quad (40)$$

Next, we truncate the series (40) to first order. This approximation is poorer than the others; at a 3/3/3 level of error in quad mod and demod, the error committed by truncation is 5–10% over most of the signal power range, rising to about 20% for very low input power, with most of it due to the dc offsets. The truncation error decreases roughly linearly with decreasing quad mod and demod errors. Finally, we substitute (2) and (37) into the truncated (40) to obtain the approximate update relation

$$\delta F(x_m, i+1) = \delta F(x_m, i) - s [p \delta F(i) + r \delta F(i)^*] - s w(i) \quad (41)$$

where

$$p = 1 + x_m |F_o|^2 \frac{G'_o}{G_o} \\ r = x_m F_o^2 \frac{G'_o}{G_o} \quad (42)$$

are level-dependent constants that determine the dynamics of  $\delta F$ , and

$$w(i) = \frac{F_o}{K v_m(i)} u(i) \quad (43)$$

is a noise term that reflects the effect of quad mod and demod errors from (38) on the predistorter error. Normally,  $p$  is close to one and  $r$  is close to zero. Because of the level dependence in (41), we will find different convergence behavior and jitter variance in the midrange, saturation, and cutoff.

We will focus on the adaptation of a specific table entry with nominal signal level  $x_m$ . In reality, a table entry represents a small range of input levels, which produces additional jitter. This effect is not included in the analysis, since it can be made arbitrarily small by increasing the number of table entries or by integrating linear interpolation with the adaptation [8]. The only remaining random variable is the phase  $\theta(i)$  of the input, which acts through the imbalance and offset errors to determine the statistics of the noise input  $w(i)$  of the iteration (41) [see (38) and (43)]. The input is therefore

$$v_m(i) = \sqrt{x_m} e^{j\theta(i)}. \quad (44)$$

As noted earlier, a table entry is updated only when the signal passes through it. These events occur at unpredictable times, typically separated by a large number of samples, so the phases  $\theta$  of the modulation signal at successive iterations can be considered independent. Further,  $\theta$  is distributed symmetrically

around the circle. Thus,  $v_m$ ,  $u$ , and  $w$  are stationary, white, zero mean processes.

We can now calculate the components of the second moments of the complex noise process  $w$ , defined as the three real quantities

$$\begin{aligned} W_{sum} &= E[|w|^2] \\ W_{diff} &= E\{\text{Re}[w^2]\} \\ W_{cr} &= E\{\text{Im}[w^2]\} \end{aligned} \quad (45)$$

where the subscripts are mnemonics for the sum of squares, difference of squares, and cross products of  $\text{Re}[w]$  and  $\text{Im}[w]$ . These definitions make  $E[w^2] = W_{diff} + jW_{sum}$ . To calculate these second moments, we substitute (38) and (44) into (43), making explicit the dependence of  $w$  on  $\theta$ . Further substitution of this result into (45) and performing the laborious expectations  $E[|w|^2]$  and  $E[w^2]$  over the  $\theta$  ensemble gives

$$\begin{aligned} W_{sum} &= |BF_o^* + bF_o|^2 + \frac{|CG_o + c|^2}{|G_o|^2 x_m} \\ &+ 2x_m \left| \frac{G_o'}{G_o} \right|^2 |F_o|^4 (|BF_o^*|^2 x_m + |C|^2) \\ &+ 2|F_o|^2 \text{Re} \left[ x_m (B^* F_o + b^* F_o^*) \frac{G_o'}{G_o} BF_o^* \right. \\ &\left. + C \frac{G_o'}{G_o} \frac{(C^* G_o^* + c^*)}{G_o^*} \right] \end{aligned} \quad (46)$$

and

$$\begin{aligned} W_{diff} + jW_{cr} &= 2 \frac{F_o^2 G_o'^2}{G_o^2} |F_o|^2 x_m (|BF_o^*|^2 x_m + |C|^2) \\ &+ 2x_m (BF_o^* + bF_o) \frac{G_o'}{G_o} B^* F_o^3 \\ &+ 2 \frac{(CG_o + c)}{G_o} \frac{G_o'}{G_o} C^* F_o^2. \end{aligned} \quad (47)$$

after use of (6) to eliminate  $K$ .

It is worth noting that numerical evaluation shows that  $W_{sum}$  is typically an order of magnitude greater than  $W_{diff}$  and  $W_{cr}$ , so that the noise  $w$  can be described approximately by its variance  $E[|w|^2]$ , without dependence on its phase angle (i.e., it is almost circularly complex). Further,  $W_{sum}$  is well approximated by the first two terms of (46), to about 3% at a 3/3/3 level of simultaneous quad mod and demod errors. These approximations are equivalent to ignoring the derivative  $G_o'$ , as explored in Section IV-E.

From (41) and the fact that  $w$  has zero mean, it would appear that  $\delta F$  also has a zero mean; that is, the iteration is unbiased. However, the dominant omitted term in the series (40) has a nonzero mean, as shown by (47), so that there is some bias in  $\delta F$ . Fortunately, the bias, as a fraction of  $F_o$ , is very small. Even at a 3/3/3 level of error in both quad mod and demod, the fractional bias is on the order of  $10^{-4}$  over most of the power range, rising to just over  $10^{-3}$  at very low input powers near cutoff. At a 1/1/1 level of error, the bias is about an order of magnitude smaller still.

In summary, the linearized iteration (41) is a good approximation to the true iteration over most of the input power range, even at the relatively high 3/3/3 level of error in both quad mod and demod. Further, the noise input  $w(i)$  is white, zero

mean, and almost circularly complex, and the bias in  $\delta F$  is negligible. At very low input powers, the approximations are somewhat degraded, though still acceptable; in any case, low input powers make a relatively small contribution to the error at the amplifier output.

### C. Jitter in $\delta F$

Now that we have the statistics of the noise input of (41), we can determine the effect on the predistorter error  $\delta F$ . Its second moments at steady state are defined as

$$\begin{aligned} F_{sum} &= E[|\delta F|^2] \\ F_{diff} &= E\{\text{Re}[\delta F^2]\} \\ F_{cr} &= E\{\text{Im}[\delta F^2]\} \end{aligned} \quad (48)$$

so that  $E[\delta F^2] = F_{diff} + jF_{cr}$ . We calculate them by forming the square and the squared magnitude of (41), taking the expectation and equating the second moments of  $\delta F(x_m, k+1)$  and  $\delta F(x_m, k)$ . After collecting terms, the result can be expressed as

$$(2\mathbf{D} - s\mathbf{E})\mathbf{F} = s\mathbf{W} \quad (49)$$

where the vectors  $\mathbf{F}$  and  $\mathbf{W}$  are  $(F_{sum}, F_{diff}, F_{cr})^T$  and  $(W_{sum}, W_{diff}, W_{cr})^T$ , respectively, and the matrices  $\mathbf{D}$  and  $\mathbf{E}$  are given by

$$\mathbf{D} = \begin{bmatrix} \text{Re}[p] & \text{Re}[r] & \text{Im}[r] \\ \text{Re}[r] & \text{Re}[p] & -\text{Im}[p] \\ \text{Im}[r] & \text{Im}[p] & \text{Re}[p] \end{bmatrix} \quad (50)$$

and

$$\mathbf{E} = \begin{bmatrix} |p|^2 + |r|^2 & 2\text{Re}[pr^*] & 2\text{Im}[p^*r] \\ 2\text{Re}[pr] & \text{Re}[p^2 + r^2] & \text{Im}[r^2 - p^2] \\ 2\text{Im}[pr] & \text{Im}[p^2 + r^2] & \text{Re}[p^2 - r^2] \end{bmatrix}. \quad (51)$$

Solution of (49) gives the desired second moments of  $\delta F$ —that is, the jitter variances.

### D. Amplifier Output Error

Having obtained the predistorter jitter, we turn to our ultimate objective, the error power in the amplifier output. In (30), we distinguished output error due to predistorter misadjustment from output error due to quad mod error, and the remainder of Section III dealt with the second component alone. In this section, we deal with the first component, the error  $v_{aeF}$  (31) due to jitter in the misadjustment  $\delta F$ . Taking the expectation of  $x_{aeF} = |v_{aeF}|^2$  over the  $\theta$  ensemble and using (42), we have

$$\begin{aligned} \bar{x}_{aeF} &= x_m \frac{K^2}{|F_o|^2} \{ (|p|^2 + |r|^2) F_{sum} \\ &+ 2\text{Re}[pr^*(F_{diff} + jF_{cr})] \}. \end{aligned} \quad (52)$$

This is the amplifier output error due to predistorter jitter, as a function of quad mod and demod errors, amplifier characteristics, signal level, and the iteration step size parameter. It can be used to obtain the convergence speed achievable at a particular predistorter table entry for any level of quad mod and demod error and a given level of allowable output error.

In the normal case of variable input level due to modulation, we average (52) to produce the average output error power due to predistorter jitter as

$$P_{aeF} = \int_0^\infty \overline{x_{aeF}(x_m) p_m(x_m)} dx_m \quad (53)$$

where  $p_m(x_m)$  is the pdf of the level of the modulated input signal.

### E. Simple Approximation

Although (52) and (53) are readily evaluated numerically, the expressions are complex enough to defeat intuition. Fortunately, a further approximation gives a very simple result, without dramatically increasing the error. We simply ignore the shift in operating point of the amplifier with respect to perturbations in the predistorter or quad mod. This is equivalent to setting the derivative  $G'_o$  to zero. From (46) and (47), we then have  $W_{diff} \approx 0$ ,  $W_{cr} \approx 0$  and the variance of the noise input  $w$  to the iteration (41) is just

$$W_{sum} \approx |BF_o^* + bF_o|^2 + \frac{|CG_o + c|^2}{|G_o|^2 x_m}. \quad (54)$$

The iteration (41) simplifies to

$$\delta F(x_m, i+1) = (1-s)\delta F(x_m, i) - sw(i) \quad (55)$$

since  $p = 1$  and  $r = 0$ , and (31) becomes

$$v_{aeF} = v_m G_o \delta F. \quad (56)$$

The solution for steady-state jitter variance  $F_{sum}$  is simple. We take the squared magnitude of (55), perform the expectation and equate the variances of  $\delta F(x_m, k+1)$  and  $\delta F(x_m, k)$  to obtain

$$F_{sum} \approx \frac{s}{2-s} W_{sum}. \quad (57)$$

$F_{diff}$  and  $F_{cr}$  are both zero. The “time constant” of the adaptation (55), measured in iterations, is

$$N_c = \frac{-1}{\ln(1-s)} \approx \frac{1}{s}. \quad (58)$$

Finally, jitter-induced output error power is, from (54), (56), and (57)

$$\bar{x}_{aeF} \approx \frac{s}{2-s} (x_m |G_o|^2 |BF_o^* + bF_o|^2 + |CG_o + c|^2) \quad (59)$$

at any level  $x_m$ . To obtain the average jitter-induced power  $P_{aeF}$ , we average (59) with respect to the modulation pdf, as in (53). If we ignore the variation of  $F_o$  and  $G_o$  with level, the average is obtained simply as

$$P_{aeF} \approx \frac{s}{2-s} \left( P_a \left| B \frac{F_o^*}{F_o} + b \right|^2 + |CG_o + c|^2 \right) \quad (60)$$

and the fractional output error power is

$$\frac{P_{aeF}}{P_a} \approx \frac{s}{2-s} \left( \left| B \frac{F_o^*}{F_o} + b \right|^2 + \frac{|CG_o + c|^2}{P_a} \right). \quad (61)$$

These results lend themselves to simple interpretation. If the quad mod is perfect ( $B = C = 0$ ) then the fractional amplifier output error power is  $(ISR_d + DSR_d)/2N_c$ , assuming the test tone used to measure the suppression ratios has the same power  $P_m$  as the data signal. If the quad demod is perfect ( $b = c = 0$ ), then the fractional amplifier output error power is  $(ISR_m + DSR_m)/2N_c$ . If both devices are imperfect, there is some chance that their errors in (60) will cancel. More likely, they will combine unhelpfully, but best case and worst case bounds are easily obtained.

Evidently, we can define an error figure (EF) for the quadrature modulator and demodulator as

$$EF = ISR + DSR. \quad (62)$$

As noted in Section II-D, the EF is the sum of the powers of the unwanted sideband image and dc tone relative to the power of an input offset tone. In Section III-B, we saw that spectral regrowth is proportional to the components of the EF and, as noted above, jitter-induced error power at the amplifier output is proportional to the EF. It is gratifying to see several forms of error power depend in a straightforward way on easily measured properties of the quad mod and demod.

We note from (60) that the required time constant increases as the EF of the quad mod and demod, that is, as the square of the imbalances and dc offsets. This has significant consequences for the initial convergence of the predistorter. Even at a 1/1/1 level, which represents the limits of good analog design without DSP compensation, at least 100 iterations are required to bring the fractional amplifier output error power to  $10^{-6}$ . Moreover, every level of the predistorter must have been exercised this often to avoid partial convergence of some levels and consequent high levels of IM. Since some random data levels have relatively low probability, there is a strong argument for use of a special training sequence during initial convergence.

We also note from (60) that there is a difference in effect between the imbalances and the dc offset. Gain and phase imbalances produce an output error with power approximately proportional to the input power  $P_m$  (ignoring changes in amplifier gain  $G_o$ ). The error due to dc offset, on the other hand, is approximately constant (again ignoring changes in amplifier gain  $G_o$ ). The consequences can be seen in (61): backing off the input power to the amplifier has almost no effect on the fractional error power at the output due to imbalances; even worse, backing off causes the fractional error power due to dc offsets to increase. Both behaviors are much worse than the classical 2-dB reduction in fractional error power for every 1-dB reduction in input power seen in third-order IM.

### F. Numerical Results

Several first-order approximations were made in obtaining the fractional amplifier output error through linearized analysis (52), and more were made in arriving at the simplified model (59). As a check on the accuracy, therefore, we compare these results with a simulated adaptation in which the input level  $x_m$  is fixed and the phase of successive inputs is

TABLE I  
SIMULATION PARAMETER SETS:  $\epsilon$ , FRACTIONAL AMPLITUDE IMBALANCE;  $\phi$ , PHASE IMBALANCE  
IN RADIANS;  $C$ ,  $c$ , dc OFFSETS RELATIVE TO UNITY FULL SCALE

Parameter Set #1		$K = 0.8$	$s = 0.01$
$\epsilon_m = 0.03$	$\phi_m = 0.03$	$C = 0.01 + 0.02j$	
$\epsilon_d = 0.03$	$\phi_d = -0.03$	$c = 0.02 - 0.01j$	
Parameter Set #2		$K = 0.8$	$s = 0.01$
$\epsilon_m = 0.01$	$\phi_m = 0.01$	$C = 0.0033 + 0.0066j$	
$\epsilon_d = 0.01$	$\phi_d = -0.01$	$c = 0.0066 - 0.0033j$	
Parameter Set #3		$K = 0.8$	$s = 0.1$
$\epsilon_m = 0.01$	$\phi_m = -0.01$	$C = 0.0033 + 0.0066j$	
$\epsilon_d = 0.01$	$\phi_d = -0.01$	$c = -0.0066 + 0.0033j$	
Parameter Set #4		$K = 0.8$	$s = 0.1$
$\epsilon_m = 0.01$	$\phi_m = -0.01$	$C = 0$	
$\epsilon_d = 0.01$	$\phi_d = -0.01$	$c = 0$	

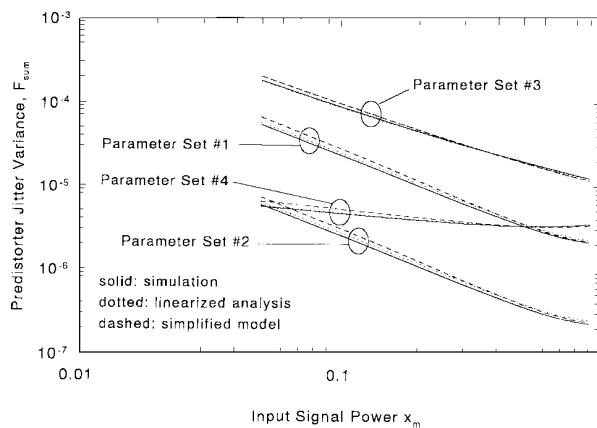


Fig. 7. Predistorter jitter variance as a function of input level.

uniformly distributed around the circle over 140 000 iterations. As benchmarks, we use the four parameter sets summarized in Table I. Parameter set 1 is at the 3/3/2.2 level of quad mod and demod error, with a 100 iteration time constant. Parameter set 2 is identical to set 1, but scaled uniformly by a factor of 3, bringing it to the 1/1/0.75 level. Parameter set 3 is a new set of values at the 1/1/0.75 level, but with a ten-iteration time constant. Finally, parameter set 4 has the same imbalance values as set 3, but has no dc offsets, putting it at the 1/1/0 level.

Fig. 7 shows the jitter variance  $E[|\delta F|^2]$  as a function of input level. There is excellent agreement between the simulation and the linearized analysis [from (49)] for all four parameter sets, and even the simplified analysis (57) is very close to both the simulation and the linearized analysis. Fig. 8 shows the output error power as a function of input level. The linearized analysis is in good agreement with the simulation on parameter set 1, at the 3/3/2.2 level, and it is almost

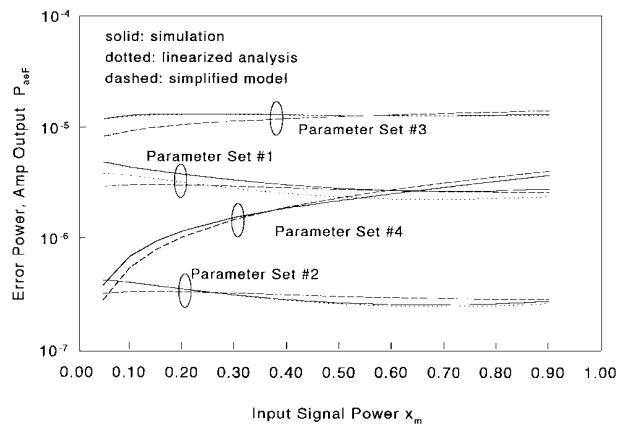


Fig. 8. Jitter-induced IM power at amplifier output as a function of input level.

indistinguishable from the simulation on parameter sets 2–4, at the 1/1/0.75 and 1/1/0 levels. Any discrepancy is due largely to truncation of the series (40). The simplified model (59), which ignores changes in amplifier gain by setting the derivative  $G'_o$  to zero, is in good agreement with both simulation and linearized analysis on all parameter sets, and is close enough to be useful for almost all purposes. We conclude that our analysis is accurate and that we can draw reliable conclusions even from the simplified model.

Turning from accuracy to behavior, we see from Fig. 7 that the curves for sets 1–3 show an inverse dependence of jitter on signal level, which, from (54), indicates that the dc offset dominates in determining the jitter. In set 4, with no dc offset, the jitter is almost independent of signal level. Similarly, on Fig. 8 we see that the sets in which dc offset dominates have relatively constant output error power, compared with the offset-free set 4, where error power is roughly proportional to input level, as predicted by (59). By comparing sets 1 and

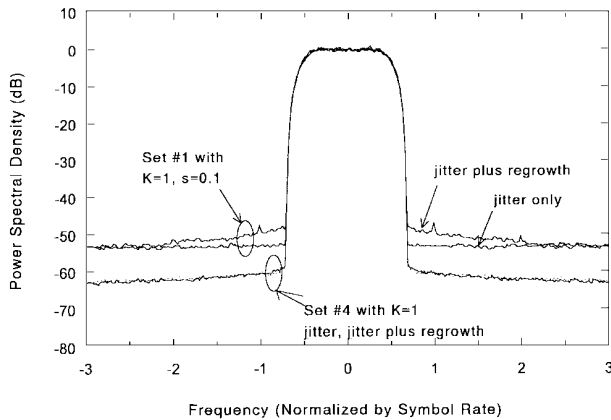


Fig. 9. Jitter-induced IM power spectra at amplifier output.

2 on Figs. 7 and 8, we also observe that the scale factor of 3 in the quad mod and demod errors produces a factor of 9 in error powers, again as predicted from (59). Finally, we note that the variances in sets 2 and 3 differ by almost two orders of magnitude, only one of which is attributable (57), (59) to the order of magnitude change in the step size parameter  $s$ . The remainder is due to the reversal of the quad demod offset  $c$ ; as noted earlier, the precise phase relationships between  $B$  and  $b$ , and between  $C$  and  $c$ , may make worst case analysis appropriate.

### G. Error Power Spectrum

In (52) and (59), we have the error power. Of more interest, however, is the error power spectrum. Here we recall from Section II-F that the iterations occur at widely separated and unpredictable times. Moreover, the levels exercised by successive input samples are unpredictable. From this, we infer that the predistorter errors at different signal levels (i.e., different table entries) are independent, which in turn implies that this component of the amplifier output error has a flat spectrum, unlike the spectral regrowth component (33). Fig. 9 illustrates the simulated spectra of the jitter-induced noise plus the spectral regrowth for parameter set 4 and for parameter set 1, the latter modified to have a ten-iteration time constant, instead of 100, and both modified for  $K = 1$ , for easier comparison with Fig. 6. The curves for jitter only (with the regrowth component removed) confirm the flat nature of the jitter spectrum. As for the total error spectrum, we see that the regrowth component is significant near the data signal spectrum for parameter set 1, but that the jitter component contributes much more total power. For parameter set 4, which is somewhat unrealistic due to its zero dc offset, the regrowth component is negligible compared with the jitter component.

Since the spectrum is flat and the fractional error does not depend on sampling rate, the ratio of power spectral densities of jitter-induced error and signal power is obtained from (61) as

$$\frac{S_{aeF}}{S_a} \approx \frac{R}{f_s} \frac{s}{2-s} \left( \left| B \frac{F_o^*}{F_o} + b \right|^2 + \frac{|CG_o + c|^2}{P_a} \right) \quad (63)$$

where  $R$  is the symbol rate and  $f_s$  is the sampling rate. This reduction by a factor equal to the number of samples per symbol implies that the quality of the output can be improved by increasing the sampling rate. However, it is computationally expensive to do so, since the reduction is only 3 dB for every doubling of the sampling rate.

Finally, we can obtain a practical design target for quadrature modulators and demodulators from (63). A typical implementation might have on the order of ten samples per symbol and would aim for  $S_{aeF}/S_a < 10^{-6}$ . It is not likely that a time constant greater than ten iterations would be acceptable. We should therefore ensure that the error figures of the quadrature modulator and demodulator satisfy

$$EF = ISR + DSR < 10^{-4}. \quad (64)$$

This simple guideline is a principal result of the paper.

## V. CONCLUSIONS

We have developed expressions for the power and power spectra of the IM error at the output of an amplifier embedded in an adaptive predistortion loop, and have included the effects of the quad mod and demod errors interacting with the adaptation algorithm and the nonlinear characteristics of the amplifier. A linearized analysis (52), (53), in which all errors are represented as small perturbations about an ideal value gives very good agreement with simulation. Even a very simple model that can be evaluated on a hand calculator (59), (60) provided sufficient accuracy for almost all purposes.

The IM error signal at the amplifier output (30) can be expressed as the sum of a component due to quad mod error with a perfect predistorter, which results in regrowth of the original IM spectrum (Section II-B), and a component due to predistorter jitter with a perfect quad mod, which results in a flat IM spectrum (Section IV-G). Both are proportional to the image suppression ratio and dc suppression ratio of the quad mod and quad demod—easily measured characteristics—which we combine to form the error figure (EF) of the devices (62).

The jitter and the corresponding flat component of the error at the amplifier output can be reduced by slowing the adaptation, that is, increasing its time constant. However, the required time constant increases linearly with the EF, that is, with the squared offsets and imbalances, and very long time constants are required even at EF levels characteristic of good analog design. The EF should not exceed  $10^{-4}$  for tolerable adaptation times (Section IV-G). Since adaptation iterations of a given table entry occur at infrequent and unpredictable times with random data, initial convergence may need a training sequence.

Backing off the amplifier input level is of no help in reducing the spectrally flat (i.e., jitter-induced) component of IM error. Relative to the signal level, the part due to gain and phase imbalances remains constant, and the part due to dc offset actually increases. Increasing the sampling rate does lower the flat spectrum, but only by 3 dB for every doubling of sampling rate.

Clearly, good design of the quad mod and quad demod, including DSP-based correction of their errors, is of primary importance in digital predistortion.

#### APPENDIX

Convergence of the basic iteration (17) at a specific  $x_m$  can be determined by representing  $F(x_m, i) = F_o(x_m) + \delta F(x_m, i)$  and expanding the denominator in a series. For small perturbations  $\delta F$ , we have

$$\begin{aligned} G[x_m|F_o + \delta F(x_m, i)|^2] \\ \approx G\{x_m|F_o|^2 + 2x_m \operatorname{Re}[F_o^* \delta F(x_m, i)]\} \\ \approx G_o + 2x_m G_o' \operatorname{Re}[F_o^* \delta F(x_m, i)]. \end{aligned} \quad (\text{A1})$$

Substitution into (17) and keeping first-order terms gives

$$\delta F(x_m, i+1) \approx -2x_m \frac{F_o G_o'}{G_o} \operatorname{Re}[F_o^* \delta F(x_m, i)]. \quad (\text{A2})$$

Taking the magnitude of both sides and bounding  $|\operatorname{Re}[F_o^* \delta F(x_m, i)]|$  by  $|F_o| |\delta F(x_m, i)|$  gives a sufficient condition for convergence in the neighborhood of the root as

$$2Kx_m \frac{|F_o| |G_o'|}{|G_o|^2} < 1. \quad (\text{A3})$$

Turning to the modified iteration (21), we use (1) and rewrite it as

$$F(x_m, i+1) = F(x_m, i)(1-s) + s \frac{K}{G[x_m|F(x_m, i)|^2]}. \quad (\text{A4})$$

Substituting  $F = F_o + \delta F$  and applying the same approximations as above, we obtain

$$\begin{aligned} \delta F(x_m, i+1) \approx (1-s)\delta F(x_m, i) - 2sx_m \frac{F_o G_o'}{G_o} \\ \cdot \operatorname{Re}[F_o^* \delta F(x_m, i)]. \end{aligned} \quad (\text{A5})$$

From this, we see that (A3) is a sufficient condition for convergence, irrespective of the value of  $s$  in  $(0, 1]$ .

#### ACKNOWLEDGMENT

The author wishes to thank the anonymous reviewers whose perceptive comments strengthened this paper.

#### REFERENCES

- [1] M. Faulkner and T. Mattsson, "Spectral sensitivity of power amplifiers to quadrature modulator misalignment," *IEEE Trans. Veh. Technol.*, vol. 41, pp. 516–525, Nov. 1992.
- [2] J. K. Cavers and M. Liao, "Adaptive compensation for imbalance and offset losses in direct conversion transceivers," *IEEE Trans. Veh. Technol.*, vol. 42, pp. 581–588, Nov. 1993.
- [3] I. K. Lau, C. G. Englefield, and P. A. Goud, "Innovative DSP implementation of adaptive RF power amplifier linearizers," in *Proc. Wireless'94*, Calgary, 1994.
- [4] J. K. Cavers, "Amplifier linearization using a digital predistorter with fast adaptation and low memory requirements," *IEEE Trans. Veh. Technol.*, vol. 39, no. 4, pp. 374–382, Nov. 1990.
- [5] B. Carnahan, H. Luther, and J. Wilkes, *Applied Numerical Methods*. New York: Wiley, 1969.
- [6] A. A. M. Saleh and J. Salz, "Adaptive linearization of power amplifiers in digital radio systems," *Bell Syst. Tech. J.*, vol. 62, no. 4, pp. 1019–1033, Apr. 1983.
- [7] A. Wright and W. Durtler, "Experimental performance of an adaptive digital linearized power amplifier," *IEEE Trans. Veh. Technol.*, vol. 41, pp. 395–400, Nov. 1992.
- [8] M. Faulkner and M. Johansson, "Adaptive linearization using predistortion—Experimental results," *IEEE Trans. Veh. Technol.*, vol. 43, pp. 323–332, May 1994.
- [9] L. Sundstrom, M. Faulkner, and M. Johansson, "Effects of reconstruction filters in digital predistortion linearizers for RF power amplifiers," *IEEE Trans. Veh. Technol.*, vol. 44, no. 1, Feb. 1995.
- [10] J. K. Cavers, "The effect of data modulation format on intermodulation power in nonlinear amplifiers," in *Proc. IEEE Veh. Technol. Conf.*, Stockholm, Sweden, May 1994, pp. 489–493.



**James K. Cavers** (M'90) was born in Port Alice, B.C., Canada, in 1944. He received the B.A.Sc. degree in engineering physics in 1966 and the Ph.D. degree in electrical engineering in 1970, both from the University of British Columbia.

From 1970 to 1979, he was an Assistant, then Associate Professor in the Department of Systems Engineering at Carleton University in Ottawa, Ont., Canada. He spent 1979 to 1982 as a Program Manager at MacDonald Dettwiler and Associates in Vancouver, B.C., Canada, followed by a year as Senior Engineer at Glenayre Electronics, also in Vancouver. In 1983, he joined the School of Engineering Science at Simon Fraser University, Burnaby, Canada, where he holds the rank of Professor. His research interests include modulation and protocols for mobile communications and integrated RF/DSP design.

Dr. Cavers is a Fellow of the Advanced Systems Institute of British Columbia, the 1992 recipient of the Stentor Telecommunications Research Award, and the 1995 recipient of the Gold Medal in Engineering and Applied Science from the Science Council of British Columbia.